

Optical trapping of spermatozoa using Laguerre-Gaussian laser modes

Raktim Dasgupta
Sunita Ahlawat
Ravi Shanker Verma
Sunita Shukla
Pradeep Kumar Gupta

Raja Ramanna Centre for Advanced Technology
Laser Biomedical Applications and Instrumentation
Division
Indore-452013, India

Abstract. We report results of a study on the use of Laguerre-Gaussian (LG) modes for optical trapping of spermatozoa. The results show that for a given trap beam power the first-order LG mode (LG_{01}) leads to lower photodamage to the cells without compromising the trapping efficiency.
© 2010 Society of Photo-Optical Instrumentation Engineers. [DOI: 10.1117/1.3526362]

Keywords: laser applications; cells; laser-induced damage; Gaussian beams.

Paper 10278RR received May 25, 2010; revised manuscript received Oct. 21, 2010; accepted for publication Nov. 1, 2010; published online Dec. 17, 2010.

Optical tweezers¹ are being used for measurements on the motility of spermatozoa²⁻⁴ and for *in vitro* fertilization by facilitating selective transport of individual spermatozoon to oocytes.⁵ To minimize possible damage to the cells due to exposure to the high light intensity (\sim hundreds of $MW\ cm^{-2}$) at the trap focus, lasers in near-IR region (wavelength $\sim 1\ \mu m$), where the absorption of the cellular components is minimal, are used. However, even at 1064 nm, negative effects of laser exposure on spermatozoa have been reported,⁶ which originate presumably from the nonlinear light absorption.⁷ Studies on the use of Laguerre-Gaussian (LG) laser modes that have a dark spot at the centre (optical vortex), for trapping of microscopic objects, have shown that compared to the TEM_{00} mode, the LG_{01} mode leads to an improved axial⁸ and transverse⁹ trapping efficiency. This has been attributed to the fact that optical trapping force is primarily contributed by the off-axis large conic angle rays. The use of an LG laser beam may therefore enable efficient trapping of the motile spermatozoa while the absence of strong axial intensity and redistribution of power into the doughnut-like region may help minimize the possible photodamage. We have therefore investigated the use of LG modes for manipulation of spermatozoa. The results obtained confirm that as compared to TEM_{00} Gaussian mode, the use of the LG_{01} mode leads to significantly lower photodamage for similar trapping efficiency.

The optical tweezers setup consists of a frequency-doubled Nd:YVO₄ laser emitting at 532 nm (Verdi-5, Coherent Inc). Note here that the major motivation for the work described in this paper is to investigate the relative efficacy of the use of LG modes and TEM_{00} Gaussian mode for the trapping of spermatozoa. We, therefore, chose 532 nm as the trap wavelength, since significant photodamage expected at this wavelength would facilitate a comparative evaluation of photodamage caused by different trap beam profiles. The linearly polarized cw Gaussian beam from the laser was phase modulated by a spatial light modulator (SLM, LCR-2500, Holoeye) to generate different orders (azimuthal indices) of LG modes. The polarization of the incoming light to the SLM was adjusted using a half-wave plate such that the SLM acts as a phase shifter. The diffracted first order was

directed onto a high-numerical-aperture (NA) microscope objective lens (Zeiss Plan-Neofluor 100 \times , 1.3) to form the optical trap. A three-lens zoom assembly was used to size the different orders of laser beams to fill $\sim 80\%$ of the objective entrance aperture. A left circularly polarized state was chosen for the trap laser beam using a polarizer and quarter-wave plate combination placed after the SLM. A halogen illumination source (12 V, 100 W) and a 50-W high-pressure mercury arc lamp, equipped with suitable bandpass filters, were used for brightfield imaging and fluorescence illumination of the sample, respectively. The brightfield images and DPH fluorescence was observed with a monochrome CCD camera (DC350F, Leica) and color images of acridine orange stained cells were observed using a color CCD camera (Watec Inc). Filters were used to suppress the back-scattered laser light and fluorescence excitation bands.

Goat testes were collected from local abattoir. Spermatozoa were collected from the cauda epididymis by retrograde flushing into the pre warmed ($\sim 37^\circ C$) media [1 mg of bovine serum albumin (BSA) per 1 mL of Biggers, Whittens, and Whittingham (BWW) medium²]. The preceding suspension was filtered through a nylon mesh filter and thereafter centrifuged (at 2000 rpm for 10 min). Finally, the spermatozoa were resuspended in BWW. The sample and buffer medium used for the experiments were then kept at $37^\circ C$. The average size of the paddle-shaped head of a goat spermatozoon estimated from brightfield microscope images was $\sim 8 \times 3.5 \times 1.7\ \mu m$ (length \times width \times thickness). For vital staining of spermatozoa, propidium iodide (PI) was used. A stock solution of 0.5-mg PI/ml of water was prepared and stored frozen at $-20^\circ C$ in the dark. The stock solution was added at the time of experiments into the spermatozoa samples so that the final concentration was $5\ \mu g/ml$. The suspension was incubated for 5 min at room temperature ($\sim 25^\circ C$). Laser-exposure-induced DNA damage to the spermatozoa was monitored using acridine orange (AO) staining. AO exhibits green and red fluorescence depending on whether it intercalates into double-stranded nucleic acids (DNA) or single-stranded nucleic acids (damaged DNA and RNA), respectively. For staining the spermatozoa with AO, the sperm chromatin structure assay method^{10,11} was used.

To assess two-photon effects that can be caused by the LG_{01} and TEM_{00} trapping beams a fluorescent probe DPH was used. DPH suspension ($\sim 4\ mM$) was prepared by dissolving it in

Address all correspondence to: Raktim Dasgupta, Raja Ramanna Centre for Advanced Technology, Laser Biomedical Applications and Instrumentation Division, Indore-452013, India. Tel: 91-731-248-8427; Fax: 91-731-248-8425; E-mail: raktim@rrcat.gov.in.

dimethyl sulphoxide (DMSO). Since DPH has minimum absorption above 400 nm, direct single-photon excitation of the probe molecules from the 532-nm laser beam is unlikely. It has its strongest absorption bands in the region 300 to 400 nm and has weak absorption¹² in the spectral region ~240 to 270 nm. The fluorescence emission could be observed using long-pass filter having transmission above 400 nm.

To estimate the efficiency of different laser modes to capture spermatozoa, video data were recorded for about 1 h, and during that period, speeds of the moving spermatozoa that could be captured by the different trapping laser modes were estimated. In our study, only spermatozoa that have fairly straight trajectories were considered. Therefore, the difference between curvilinear velocity (VCL) and straight line velocity (VSL) could be minimized for the cells analyzed in our study. The VSL of a moving spermatozoon could be estimated by noting its initial and final positions. A spermatozoon of interest was observed for ~1 to 2 s before trapping. Nearly 50 cells were studied with each type of trap. From these measurements, we estimated for each mode the maximum VSL of the spermatozoa that could just be trapped. For this, we selected five cells with highest VSL from the ~50 cells on which measurement was made. The mean and standard deviation of these are plotted in Fig. 1. From Fig. 1 we can see that as compared to a TEM₀₀ beam, the LG₀₁ beam can trap spermatozoa swimming at a higher speed. However, the third- and fifth-order LG beams fared worse than the TEM₀₀ beam. The observation is consistent with earlier reports that while using the LG₀₁ mode, the transverse trapping efficiency increases, higher order LG modes lead to a reduction in transverse trapping efficiency.⁵ The difference in the VSL of spermatozoa that could be trapped using different laser modes was found to be statistically significant with a *p* value of <0.05.

When trapped, the motile spermatozoa show strong flagellar and head motion though their position could be held constant by the trap. With increasing trapping duration the flagellar and head motion tends to die out and eventually ceased indicating

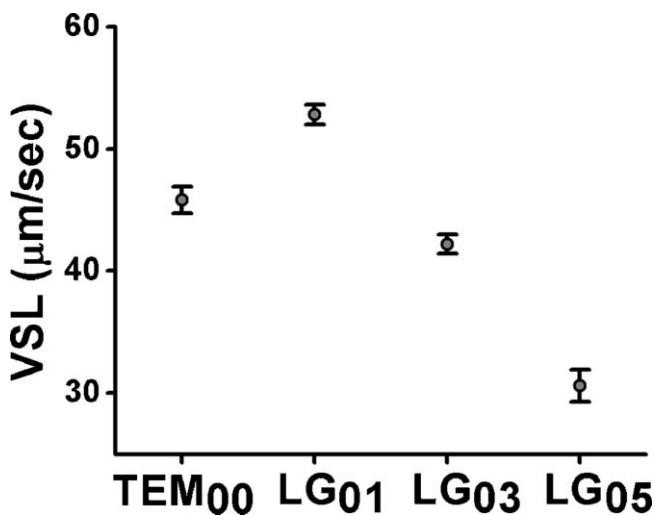


Fig. 1 Mean VSL of spermatozoa that could be just trapped by different laser modes having identical trapping power of ~140 mW at the specimen plane. The data presented are the mean \pm standard deviation. The difference in the distribution of data was found to be statistically significant, *p* < 0.05 [one way analysis of variance (ANOVA)].

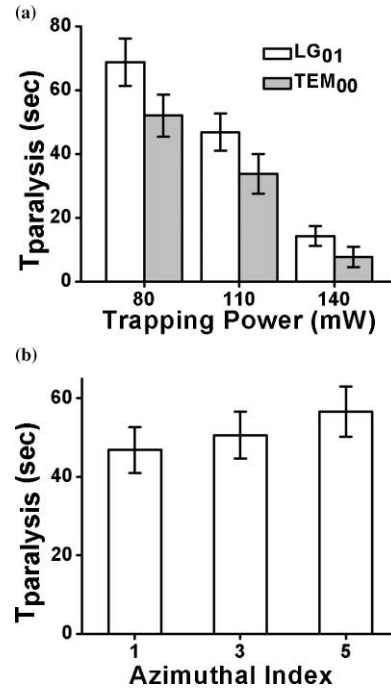


Fig. 2 (a) Time intervals $T_{\text{paralysis}}$ of the trapped spermatozoa under the TEM₀₀ and the LG₀₁ modes and (b) of the trapped spermatozoa under LG₀₁, LG₀₃, and LG₀₅ modes, each having trapping power ~110 mW. The data presented are the mean \pm standard deviation. All distributions were found to be statistically significantly different, *p* < 0.05.

a paralyzed cell. The time duration for the onset of paralysis of the cells when held continuously under optical trap can be used as an indicator for the detrimental effect of the trap. To measure the photodamage effect, the motions of the trapped cells were recorded at video rate and the time interval ($T_{\text{paralysis}}$) between the capture of the cell and the complete disappearance of any movement was noted. Figure 2(a) shows the data for the TEM₀₀ mode and the LG₀₁ mode for three trap beam power levels. A total of ~120 cells were studied for the analysis.

The measured $T_{\text{paralysis}}$ shows that cells could remain motile over a longer time as the order (azimuthal index) of the LG mode is increased [Fig. 2(b)]. The viability of the trapped cells when they turned nonmotile was further checked with PI staining. Strong PI fluorescence could be observed for most of the cells within 1 to 2 min after the cell turns nonmotile.

We used AO staining to monitor possible DNA damage in spermatozoa under the trap. The stained cells were irradiated with ~1 mW of TEM₀₀ and LG₀₁ laser profiles and evolution of AO fluorescence, when excited with 450 to 490-nm excitation, was monitored using a color CCD camera. The temporal evolution of the AO fluorescence with increasing exposure duration for the TEM₀₀ and LG₀₁ modes is shown in Fig. 3. From the CCD image data (24 bits/pixel, 8 bits for each of the red, green, and blue channels) the intensities of the green (500 to 600 nm) and red (600 to 700 nm) channels (which shows whether AO intercalates into double-stranded DNA or single-stranded DNA/RNA) were estimated. From Fig. 3(a) we can see that for low exposure times (<15 s) the red-to-green ratio is small for both the trap beams, showing very little DNA double strand breaks. However, with increasing exposure duration

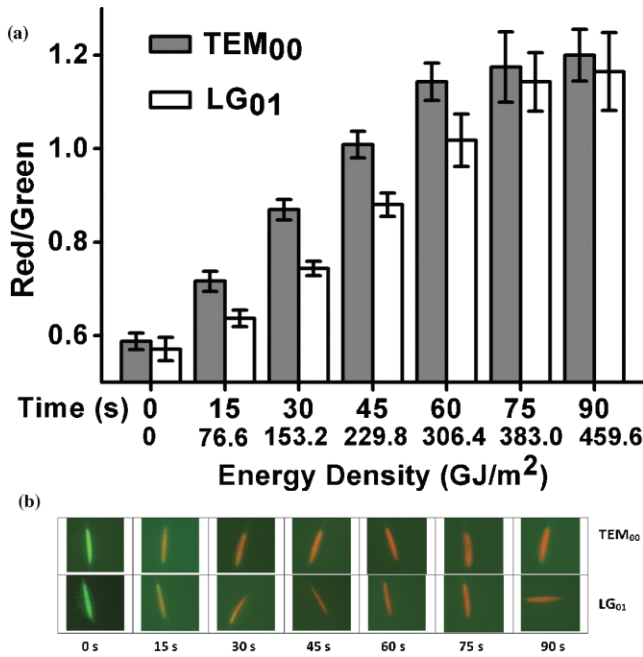


Fig. 3 Time evolution of fluorescence spectra from AO-stained spermatozoa in terms of (a) intensity ratios for the red and green channels. The data are averaged over ~ 10 cells and presented as mean \pm standard deviation. The corresponding light dosages are also shown along the time axis. The intensity ratios are statistically significantly different with $p < 0.05$ (Student's t test). (b) Time lapse images of AO-stained spermatozoa. (Color online only).

the increase in the intensity ratio occurs more quickly for the TEM₀₀ mode as compared to the LG₀₁ mode. Further, while for the TEM₀₀ mode, the intensity ratio was seen to saturate at $\sim R:G = 1.2$ within 60 s, for the LG₀₁ mode, the saturation occurred at ~ 75 s. These results suggest that the DNA damage rate is faster with the TEM₀₀ mode and implies an increased level of risk to the genetic purity of the spermatozoa. Note here that although the absorption band for AO ranges¹³ from 450 to 500 nm, it has small but nonzero absorption¹⁴ ($\sim 5\%$ of the peak value of $\sim 50,000 \text{ M}^{-1} \text{ cm}^{-1}$ at $\sim 490 \text{ nm}$) at the laser wavelength. Considering AO concentration of $\sim 15 \mu\text{M}$ used in the samples, the temperature increase at focus resulting from direct absorption of laser light by AO was estimated following the method given in Ref. 15. The estimated temperature rise is $\sim 0.004^\circ\text{C}$, which is small to cause any significant DNA damage.

It is known that due to very high power density present at the trap beam focus, significant two-photon absorption from the cw trap beam can take place, Refs. 7, 16, and 17, respectively, leading to possible damage to cell DNA having its absorption peak $\sim 260 \text{ nm}$. Therefore, the observed lower degree of DNA damage with the LG modes may be attributed to the fact that peak intensity present in an optical vortex profile is significantly lower than that of a TEM₀₀ Gaussian beam, and this can account for the observation that cells remain motile for a longer period of time with the increasing order of LG modes. To estimate the two-photon absorption for the TEM₀₀ and LG₀₁ modes, their intensity profiles at trapping plane must be determined.

It has been shown that for an optical system consisting of two media separated by a plane interface the diffracted field of the LG mode, at the point $p(r_p, \theta_p, \varphi_p)$ can be expressed as the

function of conic angle θ as^{18,19}

$$E(p) = \int_0^\alpha \int_0^{2\pi} \Psi_{m,l}(\theta) \cos \theta^{1/2} P(\theta, \phi) \exp[ik_0(r_p \kappa + \psi_d)] \times \exp(im\phi) \sin \theta \, d\theta \, d\phi, \quad (1)$$

where the origin of the coordinate system is assumed at the Gaussian focus in the absence of the aberration caused by the refractive index interface and

$$\Psi_{m,l}(\theta) = A_0 \exp\left[-\gamma^2 \frac{\sin^2 \theta}{\sin^2 \alpha}\right] \times \left(\sqrt{2}\gamma \frac{\sin \theta}{\sin \alpha}\right)^{|m|} L_l^{|m|} \left[2\gamma^2 \frac{\sin^2 \theta}{\sin^2 \alpha}\right], \quad (2)$$

and

$$\gamma = \frac{a}{w_0}, \quad (3)$$

where a is the microscope objective aperture radius, α is the largest conic angle determined by the NA of the objective lens, A_0 is the amplitude, w_0 is the beam radius at waist, and $L_l^{|m|}(x)$ are the Laguerre polynomials. Here l is the radial mode number, and m is called the azimuthal index, with $l = 0$ and $m = 0$ denoting a zeroth-order Gaussian mode (TEM₀₀); k_0 is the free space wave number of the optical beam; and $P(\theta, \varphi)$ and ψ_d represent the polarization distribution and aberration effect, respectively.¹⁸

The intensity distribution of the TEM₀₀ and higher order LG modes computed using Eq. (1) are shown in Fig. 4(a). Note that only the left circularly polarized (LCP) state is considered

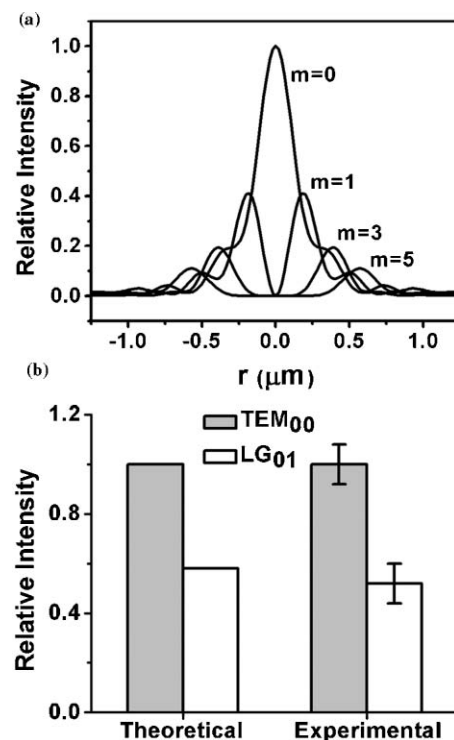


Fig. 4 (a) Intensity profiles of different laser modes and (b) estimated and observed DPH fluorescence when excited by the TEM₀₀ mode and LG₀₁ mode. The error bars indicate standard deviation of data from the mean value. The values are normalized with respect to the total fluorescence intensity estimated/observed with the TEM₀₀ mode.

for $P(\theta, \varphi)$, as the LCP state produces most symmetric intensity distribution and complete disappearance of axial intensity at the focus in the case of the LG_{01} mode.¹⁹ For identical power, the peak intensities at focus for the LG_{01} beam is $\sim 40\%$ of that produced by a TEM_{00} beam [Fig. 4(a)].

The fluorescence yield resulted from two-photon absorption can be expressed as,

$$\phi_{\text{FL},2\text{-ph}} = Q\sigma_{2\text{-ph}} \left(\frac{I}{\hbar\omega} \right)^2 N, \quad (4)$$

where $\sigma_{2\text{-ph}}$ is the mean molecular two-photon absorption cross section, $\hbar\omega$ is the photon energy, Q is the quantum yield for the dye, and N is the number of fluorophore molecules present in the excitation volume. Therefore, the ratio between total fluorescence yield with TEM_{00} and LG_{01} modes can be given as

$$\frac{(\phi_{\text{FL},2\text{-ph}})_{\text{TEM}_{00}}}{(\phi_{\text{FL},2\text{-ph}})_{\text{LG}_{01}}} = \frac{\int_x \int_y I_{\text{TEM}_{00}}^2(x, y) dx dy}{\int_x \int_y I_{\text{LG}_{01}}^2(x, y) dx dy} \quad (5)$$

To verify these estimates we measured the two-photon fluorescence yield for DPH when excited with the TEM_{00} and LG_{01} modes. The yield with the LG_{01} profile was measured to be about 52% of that with the TEM_{00} profile, which is in good agreement with the estimate of 56%. Since the probe has a very weak absorption band above 400 nm, direct excitation of the probe molecules from the laser beam due to the single-photon process is unlikely. Notably, a similar observation of reduced two-photon fluorescence from trapped dye-doped polystyrene beads was obtained by Jeffries et al.²⁰ with LG modes at 1064-nm wavelength. But with small (diameter 100 nm to 1 μm) dye-doped trapped beads, the ratio of total two-photon excited fluorescence observed for LG modes and TEM_{00} mode were much smaller ($\sim 10\%$) than observed in our studies ($\sim 50\%$). The difference likely resulted from the incomplete overlap of the annular intensity pattern of LG modes with smaller trapped beads.

Although the detailed mechanisms of cell damage due to light irradiation are not fully understood, photochemical and photothermal effects are believed to be responsible. In the UV region, light absorption by nucleic acids and proteins can result in photodamage. In the visible region, the generation of reactive oxygen species (ROSS) and free radicals produced subsequent to photoexcitation of cellular components may damage the lipid membrane, proteins, and nucleic acids through oxidative reactions.²¹ In particular, cytochromes can absorb strongly near a 532-nm laser wavelength.²² Even in the near-IR wavelengths where cellular components do not have significant absorption, photoinduced damage has been observed. While for near-IR wavelengths below 800 nm, multiphoton absorption has been shown to contribute to photodamage,^{23,24} the origin of photodamage for longer wavelengths is still poorly understood. Studies performed on spermatozoa using both cw and pulsed trap beams at 1064 nm showed much pronounced damage with short pulses for the same average power, suggesting that transient heating at the trap focus or photochemical effects resulting from multiphoton absorption may be responsible.⁶ With cw trap beams, the rise in temperature should be much smaller ($\sim 1^\circ\text{C}/100 \text{ mw}$ of trap power^{6,25}). Therefore, damage was much reduced, but for 300-mW cw power, noticeable dam-

age was present for exposure⁶ durations exceeding 2 min. The comet assay technique, which has higher sensitivity, revealed²⁶ a significant level of DNA damage to cells even when trapped for few tens of seconds using $\sim 120 \text{ mW}$ of cw laser power at 1064 nm the origin of which is not fully understood. Studies carried out on ROS generation in cells exposed to pulsed and cw 1064 nm trap beam has also provided qualitatively similar results.²⁷ While significant ROS generation in trapped cells took place with pulsed 1064-nm trap beams, with cw trap beam detectable ROS generation occurred at longer exposure times.

To conclude, the use of an optical vortex for manipulation of spermatozoa offers significant advantages in terms of reduced photodamage to the cells without compromising the trapping efficiency with the LG_{01} mode. Note that in this study, we could use trapping power of up to $\sim 140 \text{ mW}$, which was primarily limited by the diffraction efficiency and damage threshold of the SLM used for the generation of the LG modes. This power level is capable of manipulating spermatozoa having modest swimming speed ($\sim 50 \mu\text{m/s}$). For cells with higher motility, a trapping power of $\sim 500 \text{ mW}$ or more may become necessary. This can be achieved by use of diffractive optical elements offering high diffraction efficiency²⁸ or methods suitable for direct generation of high-power vortex modes in the laser cavity.²⁹

Acknowledgments

S. Shukla acknowledges the Council of Scientific and Industrial Research (Government of India) pool scheme.

References

1. A. Ashkin, "Optical trapping and manipulation of neutral particles using lasers," *Proc Natl. Acad. Sci. U.S.A.* **94**, 4853–4860 (1997).
2. J. M. Nascimento, E. L. Botvinick, L. Z. Shi, B. Durrant, and M. W. Berns, "Analysis of sperm motility using optical tweezers," *J. Biomed. Opt.* **11**, 044001 (2006).
3. B. Shao, L. Z. Shi, J. M. Nascimento, E. L. Botvinick, M. Ozkan, M. W. Berns, and S. C. Esener "High-throughput sorting and analysis of human sperm with a ring-shaped laser trap," *Biomed. Microdev.* **9**, 361–369 (2007).
4. J. M. Nascimento, L. Z. Shi, S. Meyers, P. Gagneux, N. M. Loskutoff, E. L. Botvinick, and M. W. Berns, "The use of optical tweezers to study sperm competition and motility in primates," *J. R. Soc. Interface* **5**, 297–302 (2008).
5. Y. Tadir, W. H. Wright, O. Vafa, L. H. Liaw, R. Asch, and M. W. Berns, "Micromanipulation of gametes using laser microbeams," *Hum. Reprod.* **6**, 1011–1016 (1991); B. Schopper, M. Ludwig, J. Edenfeld, S. Al-Hasani, and K. Diedrich, "Possible applications of lasers in assisted reproductive technologies," *Hum. Reprod.* **14**, 186–193 (1999).
6. Y. Liu, G. J. Sonek, M. W. Berns, and B. J. Tromberg. "Physiological monitoring of optically trapped cells: assessing the effects of confinement by 1064-nm laser tweezers using microfluorometry," *Biophys. J.* **71**, 2158–2167 (1996).
7. K. Konig, Y. Tadir, P. Patrizio, M. W. Berns, and B. J. Tromberg, "Effects of ultraviolet exposure and near infrared laser tweezers on human spermatozoa," *Hum. Reprod.* **11**, 2162–2164 (1996).
8. A. T. Oneil and M. J. Padgett, "Axial and lateral trapping efficiency of Laguerre-Gaussian modes in inverted optical tweezers," *Opt. Commun.* **193**, 45–50 (2001).
9. S. Sato, M. Ishigure, and H. Inaba, "Optical trapping and rotational manipulation of microscopic particles and biological cells using higher-order mode Nd:YAG laser beams," *Electron. Lett.* **27**, 1831–1832 (2002).
10. C. Paul, J. E. Povey, N. J. Lawrence, J. Selfridge, D. W. Melton, and P. T. K. Saunders. "Deletion of genes implicated in protecting the integrity of male germ cells has differential effects on the incidence of DNA breaks and germ cell loss," *PLoS One* **10**, e989 (2007).

11. D. P. Evenson, L. K. Jost, D. Marshall, M. J. Zinaman, E. Clegg, K. Purvis, P. de Angelis, and O. P. Claussen, "Utility of the sperm chromatin structure assay as a diagnostic and prognostic tool in the human fertility clinic," *Hum. Reprod.* **14**, 1039–1049 (1999).
12. 1,6-Diphenylhexatriene. Retrieved May 25, 2010, from <http://omlc.ogi.edu/spectra/PhotochemCAD/html/diphenylhexatriene.html>.
13. Z. Darzynkiewicz, "Differential staining of DNA and RNA in intact cells and isolated cell nuclei with acridine orange," *Meth. Cell Bio.* **33**, 285–298 (1990).
14. N. Kure, T. Sano, S. Harada, and T. Yasunaga, "Kinetics of interactions between DNA and acridine orange," *Bull. Chem. Soc. Jpn.* **61**, 643–653 (1988).
15. E. J. G. Peterman, F. Gittes, and C. F. Schmidt, "Laser-induced heating in optical traps," *Biophys. J.* **84**, 1308–1316 (2003).
16. Y. Liu, G. J. Sonek, M. W. Berns, K. König, and B. J. Tromberg, "Two-photon fluorescence excitation in continuous-wave infrared optical tweezers," *Opt. Lett.* **20**, 2246–2248 (1995).
17. K. König, H. Liang, M. W. Berns, and B. J. Tromberg, "Cell damage in near-infrared multimode optical traps as a result of multiphoton absorption," *Opt. Lett.* **21**, 1090–1092 (1996).
18. P. Török and P. R. T. Munro, "The use of Gauss-Laguerre vector beams in STED microscopy," *Opt. Express* **12**, 3605–3617 (2004).
19. S. Deng, L. Liu, Y. Cheng, R. Li, and Z. Xu "Investigation of the influence of the aberration induced by a plane interface on STED microscopy," *Opt. Express* **17**, 1714–1725 (2009).
20. G. D. M. Jeffries, J. S. Edgar, Y. Zhao, J. P. Shelby, C. Fong, and D. T. Chiu, "Using polarization shaped optical vortex traps for single-cell nanosurgery," *Nano Lett.* **7**, 415–420 (2007).
21. P. Hinterdorfer and A. van Oijen, *Handbook of Single Molecule Biophysics*, p. 71, Springer, New York (2009).
22. D. Rickwood, M. T. Wilson, and V. M. Darley-Usmar, "Quantitation and characteristics of intact mitochondria," in *Mitochondria—A Practical Approach*, V. M. Darley-Usmar, D. Rickwood, and M. T. Wilson, Eds., pp. 1–16, IRC Press, Oxford, Washington (1987).
23. H. Liang, K. T. Vu, P. Krishnan, T. C. Trang, D. Shin, S. Kimel, and M. W. Berns, "Wavelength dependence of cell cloning efficiency after optical trapping," *Biophys. J.* **70**, 1529–1533 (1996).
24. K. C. Neuman, E. H. Chadd, G. F. Liou, K. Bergman, and S. M. Block, "Characterization of photodamage to *Escherichia coli* in optical traps," *Biophys. J.* **77**, 2856–2863 (1999).
25. Y. Lui, D. K. Cheng, G. J. Sonek, M. W. Berns, C. F. Chapman, and B. J. Tromberg, "Evidence of localized cell heating induced by infrared optical tweezers," *Biophys. J.* **68**, 2137–2144 (1995).
26. S. K. Mohanty, A. Rapp, S. Monajembashi, P. K. Gupta, and K. O. Greulich, "Comet assay measurements of DNA damage in cells by laser microbeams and trapping beams with wavelengths spanning a range of 308 nm to 1064 nm," *Rad. Res.* **157**, 378–385 (2002).
27. S. K. Mohanty, M. Sharma, and P. K. Gupta, "Generation of ROS in cells on exposure to cw and pulsed near-infrared laser tweezers," *Photochem. Photobiol. Sci.* **5**, 134–139 (2006).
28. K. Sueda, G. Miyaji, N. Miyajima, and M. Nakatsuka "Laguerre-Gaussian beam generated with a multilevel spiral phase plate for high intensity laser pulses," *Opt. Express* **12**, 3548–3553 (2004).
29. J. F. Bisson, Y. Senatsky, and K. I. Ueda, "Generation of Laguerre-Gaussian modes in Nd:YAG laser using diffractive optical pumping," *Laser Phys. Lett.* **2**, 327–333 (2005).